Sliding wear behavior of Al_2O_3-NbC composites obtained by conventional and nonconventional techniques

L.R.R. Alecrim[1,2]*, J.A. Ferreira[2], C.F. Gutiérrez-González[3], M.D. Salvador[1], A. Borrell[1], E.M.J.A. Pallone[2]

[1]Instituto de Tecnología de Materiales (ITM), Universitat Politècnica de València, Camino de Vera s/n, 46022 Valencia, Spain

[2]Universidade de São Paulo/Faculdade de Zootecnia e Engenharia de Alimentos; Av. Duque de Caxias Norte, 225, 13635-900 Pirassununga-SP, Brazil

[3]Centro de Investigación en Nanomateriales y Nanotecnología (Consejo Superior de Investigaciones Científicas, Universidad de Oviedo, Principado de Asturias), Avenida de la Vega 4-6, 33940 El Entrego, Spain

*Corresponding author: Universidade de São Paulo, Av. Duque de Caxias Norte, 225, 13635-900 Pirassununga-SP, Brazil. Tel.: +34 963876230; Fax: +34 963877629
E-mail: laisribeiro@usp.br (L.R.R. Alecrim)

ABSTRACT

This study aims to investigate the dry sliding wear behavior of Al_2O_3–5vol.%NbC nanocomposite sintered by conventional and spark plasma sintering at temperatures from 1450 to 1600 ºC. The tests were performed using WC–6 wt%Co balls as a counterpart material, a load of 30 and 60 N, a sliding distance of 2000 m and a sliding speed of 0.1 m/s. The consolidation techniques influenced the friction coefficient, wear rates and patterns. Samples tested at 30 N showed better wear resistance than the samples tests with 60 N. The nanocomposites obtained by SPS at 1500 ºC exhibited a lower friction coefficient and wear rate compared to all other materials. The results indicated that Al_2O_3-NbC nanocomposites show promise as material for cutting tool applications.

Keywords: Ceramic-matrix composite; Spark Plasma Sintering; Sliding wear; Cutting tools

1. Introduction

As a material, ceramics have the potential for use in friction systems. Some ceramic phases exhibit unique properties, such as high hardness and elastic modulus, high resistance to mechanical compression, and chemical inertness, even in extreme conditions of high velocity and temperature. CBN, Si_3N_4, SiC, Al_2O_3 and ZrO_2 are examples of such materials; these characteristics are especially notable when reinforced with a second phase: Al_2O_3/TiC, Al_2O_3/Ni, Al_2O_3/Mo, and Al_2O_3/Nb [1-8]. Due to their superior properties compared to metals, these ceramic materials have attracted great interest in their potential for products that require high wear resistance, such as bearings, cutting tools, etc. For equipment operating under high mechanical contact conditions, preventing or reducing wear reduces machining costs and increases process productivity and quality [9-13].

In ceramic materials, there is a great deal of complexity involved in interaction between the intrinsic characteristics of the material and their microstructural behavior due to heating processes and wear testing conditions. It is well known that material wear can be optimized by taking different facts into consideration: (i) microstructural refinement is beneficial for wear resistance, since it delays the transition to severe wear and hence reduces the mild or moderate wear rate; (ii) the material's hardness affects the speed of introducing dislocations and thus stress accumulation at grain boundaries. In this sense, transition times towards severe wear will be higher; (iii) when toughness increases at grain boundaries, transition times to severe wear will also be increased and the severe wear rate lowered, (iv) when contact roughness decreases - for example, by lubrication or polishing - moderate wear is reduced and the transition to severe wear is slower; finally, (v) residual stress can be minimized as a consequence of the sintering process (i.e. conventional sintering vs. spark plasma sintering) [8].

The wear behavior of different ceramic carbides materials sintered using various consolidation processes has been evaluated in-situ laboratory conditions and tribosystem configurations. However, in the literature has not yet evaluated dry sliding wear in Al_2O_3-NbC bulk materials obtained by conventional (pressureless sintering) and non-conventional (spark plasma sintering, SPS) sintering techniques. Niobium carbide is widely used in cutting tools. This transition metal carbide has a high melting point, high hardness and high toughness, and low chemical reactivity. Furthermore, Al_2O_3 and NbC are thermomechanically compatible, because both materials have

similar thermal expansion coefficients, 4–9·10^{-6} K^{-1} and 5–9·10^{-6} K^{-1}, respectively. This reduces residual stresses produced during the heating and cooling processes [14,15]. This investigation aims to study the tribological behavior of Al_2O_3-NbC nanocomposites without additional sintering additives, obtained by both conventional and spark plasma sintering. The influence of the final properties and microstructural parameters, together with the sintering techniques, were tested and compared. This article discusses friction coefficient and dry sliding wear behavior, which are related to these properties, in detail.

2. Experimental procedure

2.1. Material and sintering conditions

In this study, nanometric powders of α-alumina (AKP-53, Sumitomo, 99.95% purity) and niobium carbide were obtained by reactive high-energy milling as described in a previous investigation [16,17]. The final compositions of the samples, with 5 vol.% NbC, were obtained by adding alumina to the reactive milling products. The composite mixtures were obtained in a conventional ball mill in alcohol suspension with 0.2 wt% PABA, 100 ppm magnesium chloride hexahydrate ($MgCl_2 \cdot 6H_2O$), and 0.5 wt% oleic acid. This percentage of inclusion was determined based on results obtained in research in development by the group with different amounts of inclusions of niobium carbide nanometric in the alumina matrix.

Two different nanocomposites sintering techniques were studied: (i) conventional sintering, employing a tubular furnace (Thermal Tecnology Inc – Astro Division), and (ii) spark plasma sintering (FCT Systeme GmbH, HPD25, Germany) under vacuum conditions.

For the conventional sintering (CS), Al_2O_3–5 vol.% NbC powders were isostatically compressed at 200 MPa, and the resulting pieces were fired in a tubular furnace at different temperatures (1550 and 1600 ºC) under vacuum, with heating and cooling rates of 10 ºC/min and 120 min of dwell time at the maximum temperature.

For the spark plasma sintering (SPS), cylindrical samples 20 mm in diameter were prepared as follows; (i) the samples were heated from room temperature to 600 ºC at a rate of 200 ºC/min at a pressure of 10 MPa, then heated from 600 ºC to the final temperature a heating rate of 100 ºC/min and a pressure of 80 MPa. The final temperatures were set at 1450, 1500, 1550, and 1600 ºC; these temperatures were

maintained for 5 minutes under a pressure of 80 MPa. Sintering cycles were performed under vacuum conditions.

2.2. Characterization

The densities of the consolidated materials (relative density) were measured using the Archimedes method with distilled water immersion, according to ASTM C373-88. Relative densities were estimated in accordance with the real density of the powder measured by Helium picnometry (4.10 g/cm^3). The sintered samples were fractured on their cross-sections and observed by field emission scanning electron microscopy (FESEM, Zeiss Ultra55, Polytechnic University of Valencia). The surface of the materials was polished to 0.25 μm using SiC paper and diamond suspension, and their wear tracks were observed by FESEM.

The Vickers hardness value (HV) was determined using a conventional diamond pyramid indenter, applying a 10 Kgf load for 10 s (Buehler, model Micromet 5103) according to ASTM E92-72 [18].

2.3. Sliding wear test

The wear tests were carried out under dry sliding conditions using a Microtest MT2/60/SCM/T tribometer with ball-on-disc configuration, following ASTM wear testing standard G99-03 [19]. A WC–6 wt% Co cemented carbide ball produced by FRITSCH (Germany) with a hardness of 1680 HV_{30} and 5 mm radius was used as the counter material. The tests were performed using a contact load of 30 and 60 N, a sliding speed of 0.1 m/s, a sliding distance of 2000 m, and a wear track radius of 3 mm. All tests were conducted in controlled conditions (23 ± 2 ºC room temperature and 60 ± 2% relative humidity). In order to obtain a representative value for each response parameter, a series of three tests were carried out for each material.

The sample surfaces were polished and cleaned before the wear test, achieving a surface roughness of 0.5 μm for the conventionally sintered (CS) samples and 0.1 μm for the SPS samples (Perthometer M2 – Mahr). The wear rate was calculated using equation 1 [20,21]:

$$W = \frac{V}{L \cdot P} \qquad (1)$$

where, V is the volume loss in mm^3 (determined from sample's mass loss divided by the density of each sample), L is the sliding distance in m, and P is the applied load in N. The wear mass lost was obtained by calculating the difference in mass before and after the test.

3. Results and discussion

3.1. Mechanical and microstructural characterization

Table 1 shows the values of the two important properties, density and Vickers hardness, for a complete characterization of the tribological tests of the samples sintered at different temperatures using conventional (CS) and spark plasma sintering (SPS). It is important to note that the SPS sintered samples show higher density and hardness than the samples sintered using the conventional method; this result is expected, due to application of pressure during the SPS process (80 MPa) and the high heating rates and short dwell times.

Table 1. Density and hardness of the Al_2O_3-5vol.% NbC composites sintered by CS and SPS at different temperatures.

Sintering technique	Temperatures (ºC)	Designation	Bulk density (g/cm^3)	Relative density (%)	Vickers hardness HV_{10} (Kgf/mm^2)
Conventional Sintering	1550	1550 CS	3.83	92.4 ± 0.1	2172 ± 15
	1600	1600 CS	3.90	93.8 ± 0.1	2386 ± 18
Spark Plasma Sintering	1450	1450 SPS	4.09	99.8 ± 0.1	2578 ± 13
	1500	1500 SPS	4.09	99.8 ± 0.1	2590 ± 14
	1550	1550 SPS	4.08	99.7 ± 0.1	2512 ± 12
	1600	1600 SPS	4.06	99.5 ± 0.1	2478 ± 15

Using SPS, only 1450 ºC with 5 min of dwell time was needed to achieve values approaching theoretical density; in contrast, the CS technique required a 1600 ºC temperature and 120 min of dwell time to reach value of approximate 94% of theoretical density. The non-conventional technique therefore offers economic and energy savings and improved grain growth inhibition (Fig. 1). The fracture surface of two representative materials consolidated by CS and SPS at 1550 ºC can be seen in Fig. 1. The microstructures display a homogeneous distribution of niobium carbide particles within the alumina matrix. The CS samples (Fig. 1a) show a microstructure with the average grain of less than 5 μm. Fig. 1b shows the finest microstructure with small nanoparticles of NbC (white particles) embedded in the microstructure of the alumina matrix.

3.2. Friction coefficient

The friction coefficient (μ) is the ratio between friction force and the imposed normal force. The friction force was continuously measured during the test using a load cell with a piezoelectric transducer on the loading arm. The change in friction coefficients over time normally presents two different regions, called the non-steady or running-in state and the steady state [22]. Fig. 2 presents the average of friction coefficients for the Al_2O_3–5 vol.% NbC materials tested over 2000 m of sliding distance and with 30 and 60 N of applied load. The standard deviation for all the tests performed under the same conditions was less than 5% in all cases.

In general, an initial observation shows that the behavior of the friction coefficient is strongly influenced by the load applied and the consolidation technique used. Increasing the contact load creates a general increase in the friction coefficient. The CS sintered materials show higher friction coefficient values than the SPS materials; this is due to the lower density and lower hardness values of the CS materials compared with the SPS samples (Table 1). The SPS material friction coefficients behave similarly, except the sample sintered at 1500 ºC under 30 N of contact load, which presented the lowest value of all the materials (0.15).

Another remarkable effect is the high friction coefficients seen in the samples sintered at high temperature (1550 and 1600 ºC) using both techniques and the two different load conditions. This is probably related to the influence of hardness on the friction coefficients, whereas less hard materials offer a lower friction resistance, increasing

the friction coefficient values [23]. Therefore, the materials sintered by SPS at low temperatures show a similar and regular change in friction coefficients. The generation of wear fragments (from Al_2O_3 and NbC particles, and of the WC-6Co ball) acts like a third body on the contact surface and may contribute to the higher friction coefficients. It is important to note the difference in the friction coefficient value at 60 N of contact load for the 1450 SPS sample (0.39) and the 1600 SPS sample (0.47)—an increase of 20%. This behavior is due to the finer microstructure and high hardness [24], which minimizes the formation of wear debris. Alecrim et al. [24] reported that the evolution of the microstructures of the Al_2O_3-NbC composites used in this study, where the increase of the alumina grain size is in function of the maximum sintering temperature. As the sintering temperature was increased, from 1450 to 1600 ºC, the proportion of these alumina grains increased.

3.3. Wear characteristics

The wear mechanism and the associated volumetric wear rate depend critically on the precise test conditions. In general, the materials tested in this study showed excellent wear resistance to dry sliding.

The volumetric wear rate (W) is a material characteristic that is comparable for materials used under the same conditions of wear. It is calculated using equation 1.

Fig. 3 shows the wear rate for each tested material under both load conditions and both sintering techniques. As expected, the wear rate increased at the higher contact load under otherwise equal conditions, in agreement with reported results by Bonny et al. [25].

As we see in Fig. 3, the wear rates of all composites sintered by SPS under 30 N of load are on the order of 10^{-8} $mm^3/N{\cdot}m$ while for these materials under 60 N of load the wear rate is on the order of 10^{-6} $mm^3/N{\cdot}m$, demonstrating the important influence of this parameter.

Materials sintered by SPS showed better dry sliding wear resistance compared to the conventional sintered samples. The best results of wear rate were obtained for the material sintered by SPS at 1500 ºC and tested with both applied loads. Those materials presented the lowest wear rates and showed the highest hardness values. Hardness is usually accepted as the best indicator of wear resistance. Materials with high hardness are usually more resistant. The optimal sintering conditions using the

SPS technique are the principal cause of the smaller grain sizes and consequently the improvement in hardness. Therefore, the wear resistance of materials sintered by SPS is governed by these properties, which offer resistance to pull-out of the near-nanostructured composites [21].

The influence of the heating process in samples sintered by SPS is related to the hardness increment: i.e. the difference between 1550 CS and 1550 SPS is 387 HV_{10}, and between 1600 CS and 1600 SPS it is 102 HV_{10}. Consequently, the 1550 SPS sample shows a lower wear rate (on the order of 10^{-8} $mm^3/N{\cdot}m$) compared to the 1550 CS sample (on the order of 10^{-6} $mm^3/N{\cdot}m$) under 30 N of load, which is in keeping with the lower friction coefficient value (0.34 and 0.49, respectively). With 60 N of contact load there is less difference in the friction coefficient and wear rate. Finally, at high temperatures (1600 ºC) the samples show a similar behavior in the wear properties that samples tested at 30 N.

It should be noted that the wear rates are obtained from the samples' volumetric loss and do not involve the wear of the counterpart. In this case, the governing mechanism is polishing of asperities and microabrasion of the sample surfaces.

The wear mechanism and the associated volume wear rate depend of the test conditions; the wear regimes of ceramics can be classified into two types: moderate and severe. In the moderate regime, wear rates assume values below 10^{-6} $mm^3/N{\cdot}m$, while in the several regime wear rates are greater than this value, although the boundary condition between the two systems is not precisely defined [1-2,26]. In general, all composites in this study showed excellent wear resistance to dry sliding; the samples sintered by SPS and 30 N of load show a moderate wear rate, while the CS samples under both loads and SPS under 60 N of load presented severe wear.

3.4. Wear surface analysis

The materials consolidated by CS have a lower wear resistance compared to the materials consolidated by SPS. Therefore, significant differences might be expected in observations of the wear track for materials consolidated by the two techniques.

Fig. 4 shows FESEM micrographs of the wear tracks for the CS materials at 30 N of contact load. The worn surface shows different levels of damage, which is in accordance with the wear rates obtained. The wear track analysis revealed that the wear process for the Al_2O_3–5 vol.% NbC composites obtained by CS produces smears

and relatively smooth surfaces, with some scratches and furrowing; the process is controlled by abrasion with a plastic deformation, adhesion, and tribofilm formation. The appearing of a smooth surface in the sample can identify the tribofilme formation. The debris are broken during the test by the continuous contact and friction between the two solid surfaces and, under the action of the applied load, these debris forms a film planning the surface.

In Fig. 4 the wear track shows the appearance of a wear debris layer adhered to the surface in all areas. Some wear debris can be seen appearing as bright spots over the surface, possibly as a consequence of the fragmentation of NbC grains.

Fig. 5 shows the wear track micrographs for the materials consolidated by CS under 60 N of contact load; in these we note a wear mechanism controlled by abrasion and plastic deformation behavior. The sample sintered at 1550 ºC (Fig. 5a) shows a relatively smooth surface with grain fracture and tribofilm formation, while the smooth surface of the sample sintered at 1600 ºC (Fig. 5b) provides evidence of scuffing and a binder removal. This scuffing can be explained by the dimensional change undergone by the sample in the continuous cooling-heating cycles that occur during the cyclic pulses from thermomechanical fatigue [27].

Fig. 6 shows the FESEM micrographs of the SPS sample wear tracks at 30 N, demonstrating the different levels of surface deterioration for the materials tested. These are consistent with the wear rates obtained. The worn surface of these samples shows that their wear behavior is plastic deformation, with a relatively smooth surface and a wear process controlled by abrasion and grain fracture.

Partial cracks perpendicular to the sliding direction were observed during sliding. These cracks are due to the tensile stress at the trailing edge of the contact areas. The surface of the composites was covered by compacted debris resulting from frequent microfracture events, which may be due to the sintering technique used [28]. It should be noted that the wear process is controlled by adhesion and grain pull-out, except for the sample sintered at 1450 ºC (Fig. 6a). The samples sintered at 1550 and 1600 ºC show a smeared structure, which is evidence of scuffing, as seen in Fig. 6c and Fig. 6d.

Fig. 7 shows the FESEM micrographs of the wear tracks generated at 60 N for the materials consolidated by SPS; demonstrating a wear mechanism controlled by abrasion and plastic deformation. The samples sintered at 1450 ºC and 1500 ºC (Fig. 7a and 7b) show evidence of scuffing. The wear tracks for these samples show a debris

layer. The sample sintered at 1550 ºC (Fig. 7c) presents a relatively smooth surface with a smeared structure. Note that the sample sintered at 1600 ºC (Fig. 7d) demonstrates a wear process controlled by adhesion, grain fracture and grain pull-out on the worn surface.

Observing the different wear mechanisms allows a possible sequence of surface damage to be postulated. Wear may start by means of a combination of plastic deformation and microabrasion, which in turn facilitates the removal or fracture of NbC grains. The wear debris generated may act as a third body, causing abrasion phenomena, or it may adhere to the contact surface, creating a tribofilm.

4. Conclusions

This investigation evaluated the friction and wear behavior of pressureless sintering and spark plasma sintering of Al_2O_3–5 vol.% NbC nanocomposites using a ball-on-disc tribometer with WC–6% Co balls. The data obtained reveal the following results:

1. With the application of pressure during SPS process it was possible obtain denser and harder nanocomposites than pressureless sintering, and these final properties are directly related to the improvement of the friction and wear behavior of the samples.
2. There was a relevant reduction in friction coefficient when the materials were sintered using the SPS technique. Under both contact load test conditions of 30 N and 60 N, the material obtained at 1500 ºC by SPS show the lowest friction coefficient.
3. The wear rate values were about twenty times lower for composites consolidated by SPS compared to materials sintering by CS. In general, the samples showed a moderate wear rate, except the samples sintered by CS, which presented severe wear.
4. The good sliding wear resistance of the SPS samples might be attributed to the nanoparticles of NbC embedded in the microstructure of the alumina matrix, in comparison with CS materials.
5. Damage levels observed in the wear tracks for the different materials allow us to postulate a possible sequence of surface damage: plastic deformation, grain pull-out, fracture and/or removal of particle grains, and finally abrasion and/or adhesion phenomena with tribofilm formation.

This work presents the first study of the wear behavior of Al_2O_3-NbC nanocomposites consolidated by CS and SPS; the excellent results obtained constitute a window of opportunities for the fabrication of products such as cutting tools using these materials.

Acknowledgment

This work has been financial support by the Brazilian institution CAPES for the project CAPES-PVE A086/2013 (project Nº 23038.009604/2013-12). A. Borrell acknowledges the Spanish Ministry of Economy and Competitiveness for her *Juan de la Cierva-Incorporación* contract (IJCI-2014-19839).

References

[1] Adachi K, Kato K, Chen N. Wear map of ceramics. Wear 1997;203-204:291-301.

[2] Kato K, Adachi K. Wear of advanced ceramics. Wear 2002;253:1097-1104.

[3] Wahi RP, Llschner B. Fracture behavior of composites based on Al_2O_3-TiC. J Mater Sci 1980;15:875-885.

[4] Medvedovski EE. Wear-resistant engineering ceramics. Wear 2001;249:821-828.

[5] Rainforth WM. The wear behavior of oxide ceramics-A review. J Mater Sci 2004;39:6705-6721.

[6] Tedesco NR, Pallone EMJA, Tomasi R. Effect of the pin-on-disc parameters on the wear alumina. Adv Sci Technol 2010;65:39-44.

[7] Portu Gd, Guicciard S, Melandri C, Monteverde F. Wear behavior of Al_2O_3-Mo and Al_2O_3-Nb composites. Wear 2007;262:1346-1352.

[8] Rodríguez-Suarez T, Bartolomé JF, Smirnov A, López-Esteban S, Torrecillas R, Moya JS. Sliding wear behavior of alumina/nickel nanocomposites processed by a conventional sintering route. J Eur Ceram Soc 2011;31:1389-1395.

[9] Kerkwijk B, Buizert JJ, Verweij H, Awater RH. Tribological tests verify wear resistance. Am Ceram Bull 2000;49-53.

[10] Kumar AS, Durai A R, Sornakumar T. Wear behaviour of alumina based ceramic cutting tools on machining steels. Tribol Inter 2006;39:191-197.

[11] D'errico GE, Bugliosi S, Calzavarini R, Cuppini D. Wear of advanced ceramics for tool materials. Wear 1999;225-229:267-272.

[12] Borrell A, Salvador MD, García-Rocha V, Fernández A, Chicardi E, Gotor FJ. Spark plasma sintering of $Ti_yNb_{1-y}C_xN_{1-x}$ monolithic ceramics obtained by mechanically induced self-sustaining reaction. Mater Sci Eng A 2012;543:173-179.

[13] Kumar AS, Durai AR, Sornakumar T. Wear behavior of alumina based ceramics cuuting tools on machining steels. Tribol Inter 2006;39:191-197.

[14] Pasoti RMR, Bressiani JC. Sintering of alumina-niobium carbide composite. Inter J Refract Met Hard Mater 1998;16:423-427.
[15] Acchar W, Segadães AM. Properties of sintered alumina reinforced with niobium carbide. Inter J Refract Met Hard Mater 2009;27:427-430.
[16] Pallone EMJA, Trombini V, Botta Filho FWJ, Tomasi R. Synthesis of Al_2O_3-NbC by reactive milling and production of nanocomposites. J Mat Proc Tech 2003;143-144:185-190.
[17] Botta Filho FWJ, Tomasi R, Pallone EMJA, Yavari AR. Nanostructured composites obtained by reactive milling. Scr Mater 2001; 44:1735-1740.
[18] ISO 3078-1983: Hardmetals, Vickers Hardness Test.
[19] ASTM G99-03, Standard Test Method for Wear Testing With a Pin-on-disc Apparatus, ASTM Annual Book of Standards, vol. 03.02, West Conshohocken, PA, 2003.
[20] Chen WH, Lin HT, Chen J, Nayak PK, Lee AC, Lu HH, Huang JL. Microstructure and wear behavior of spark plasma sintering sintered Al_2O_3/WC-based composite Inter J Refract Met Hard Mater 2016;54:279-283.
[21] Espinoza-Fernández L, Borrell A, Salvador MD, Gutierrez-Gonzalez CF. Sliding wear behavior of WC-Co-Cr_3C_2-VC composites fabricated by conventional and non-conventional techniques. Wear 2013;307:60-67.
[22] Fervel V, Normand B, Coddet C. Tribological behavior of plasma sprayed Al_2O_3-based cermet coatings. Wear 1999;230:70-77.
[23] Bayer RG. Mechanical Wear Fundamentals and Testing, Revised and Expanded. Second Edition, Revised and Expanded (Marcel Dekker, NY, 2004).
[24] Alecrim LRR, Ferreira JA, Gutiérrez-González CF, Salvador MD, Borrell A, Pallone EMJA. Effect of reinforcement NbC phase on the mechanical properties of Al_2O_3-NbC nanocomposites obtained by spark plasma sintering. Inter J Refract Met Hard Mater 2016, doi:10.1016/j.ijrmhm.2016.10.021.
[25] Bonny K, De Baets P, Vleugels J, Huang S, Lauwers B. Tribological characteristics of WC-Ni and WC-Co cemented carbide in dry reciprocating sliding contact. Tribol Trans 2009;52:481-491.
[26] Pasaribu HR, Sloetjes JW, Schipper DJ. The transition of mild to severe wear of ceramics. Wear 2004;256:585-591.

[27] Tuci A, Esposito L. Second phase and materials transfer in alumina ceramics sliding systems. Wear 2000;245:76-83.
[28] Borrell A, Torrecillas R, Rocha VG, Fernandez A, Bonache V, Salvador MD. Effect of CNFs content on the tribological behaviour of spark plasma sintering ceramic-CNFs composite. Wear 2012;274-275:94-99.

Figures:

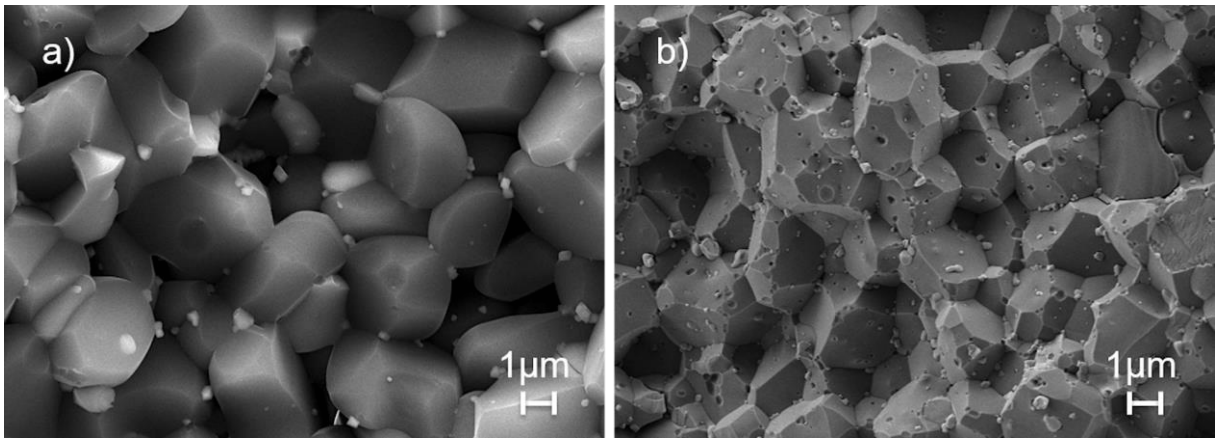

Fig. 1. FESEM micrographs of consolidated materials: (a) 1550 CS and (b) 1550 SPS.

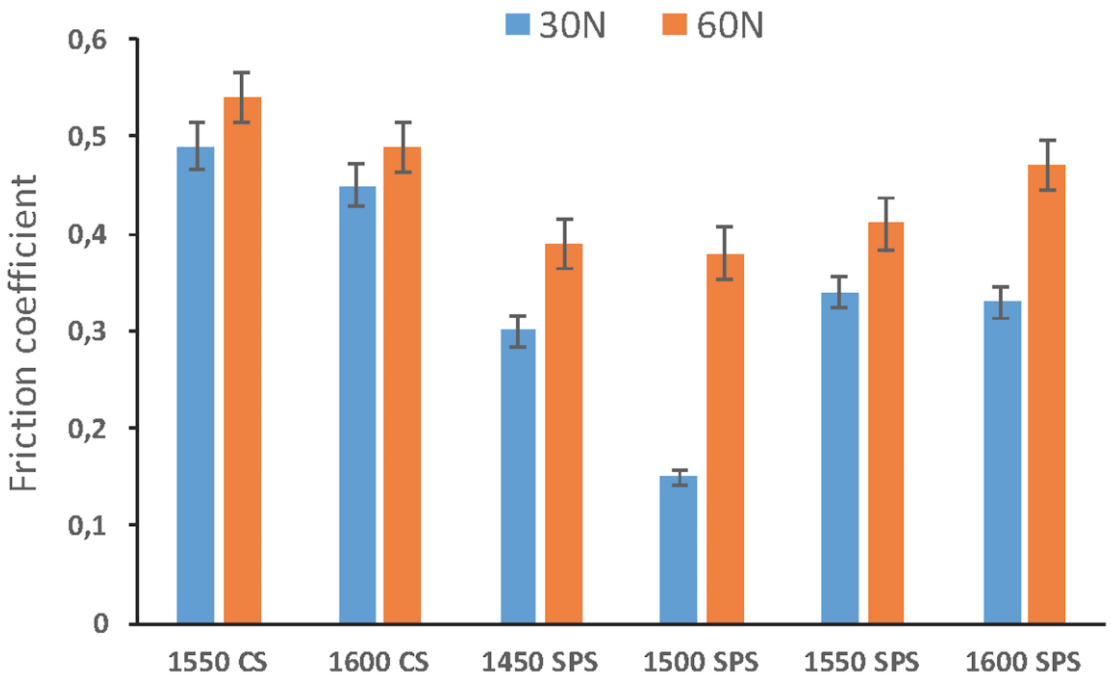

Fig. 2. Average friction coefficient of the sintered materials by CS and SPS with different contact loads.

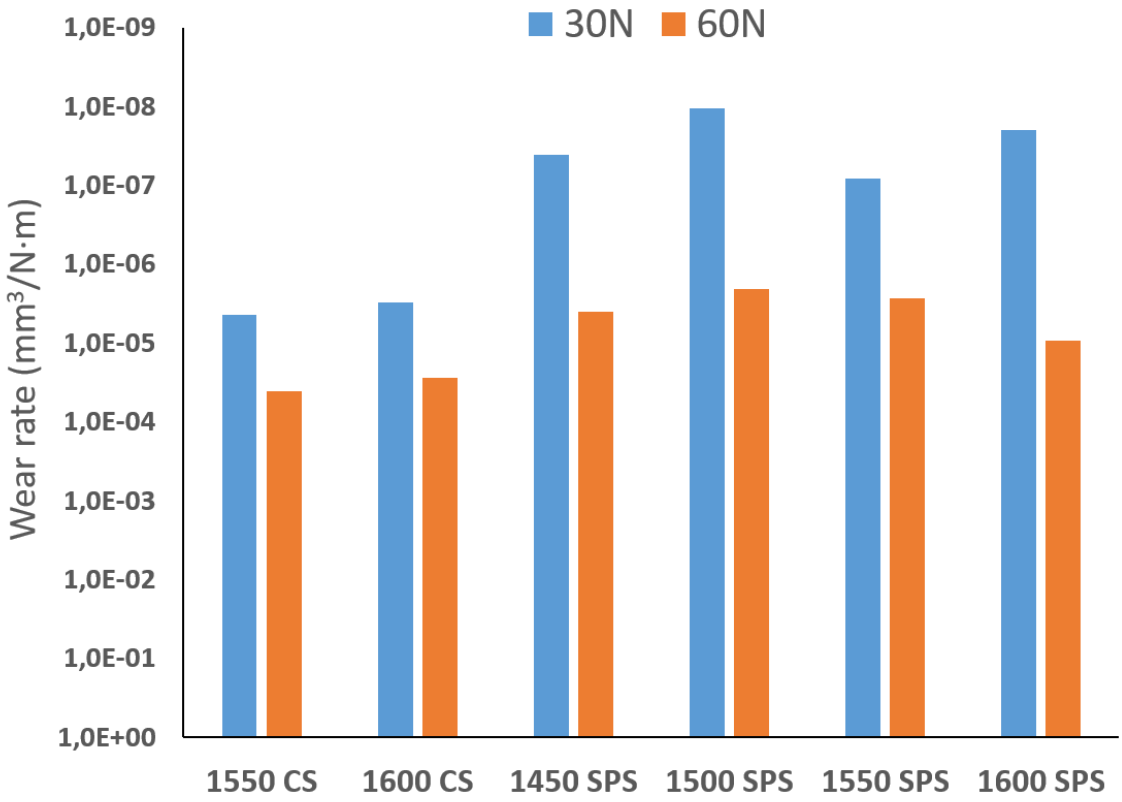

Fig. 3. Wear rate of the Al_2O_3-5vol.% NbC materials sintered by CS and SPS with different contact loads.

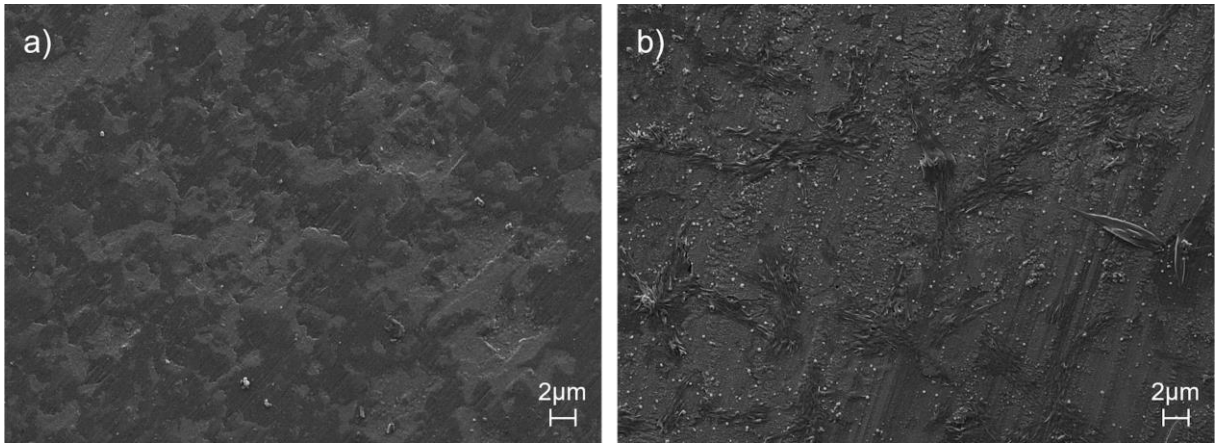

Fig. 4. FESEM micrographs of the wear tracks of Al_2O_3-5vol.% NbC composites consolidated by CS: (a) 1550 ºC and b) 1600 ºC for 30 N of contact load.

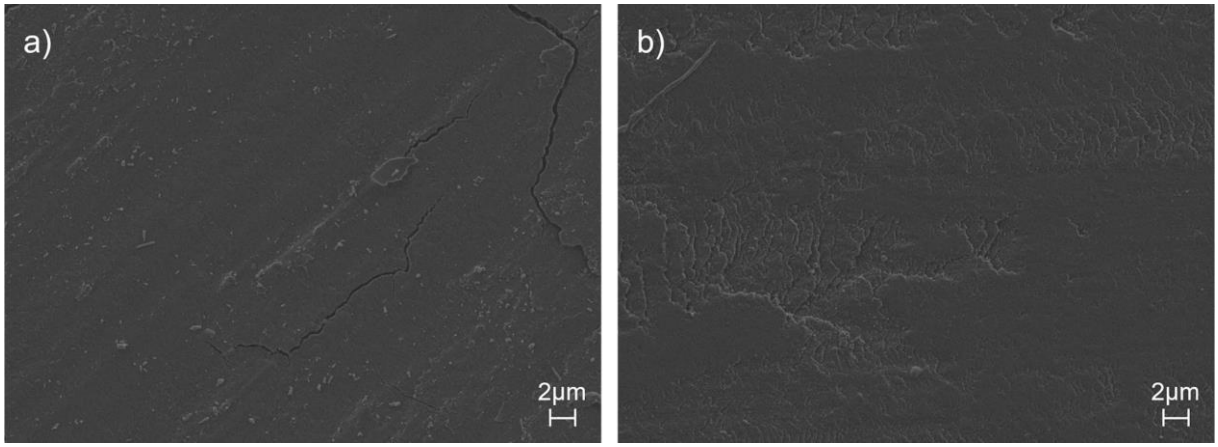

Fig. 5. FESEM micrographs of the wear tracks of Al_2O_3-5vol.% NbC composites consolidated by CS: (a) 1550 ºC and b) 1600 ºC for 60 N of contact load.

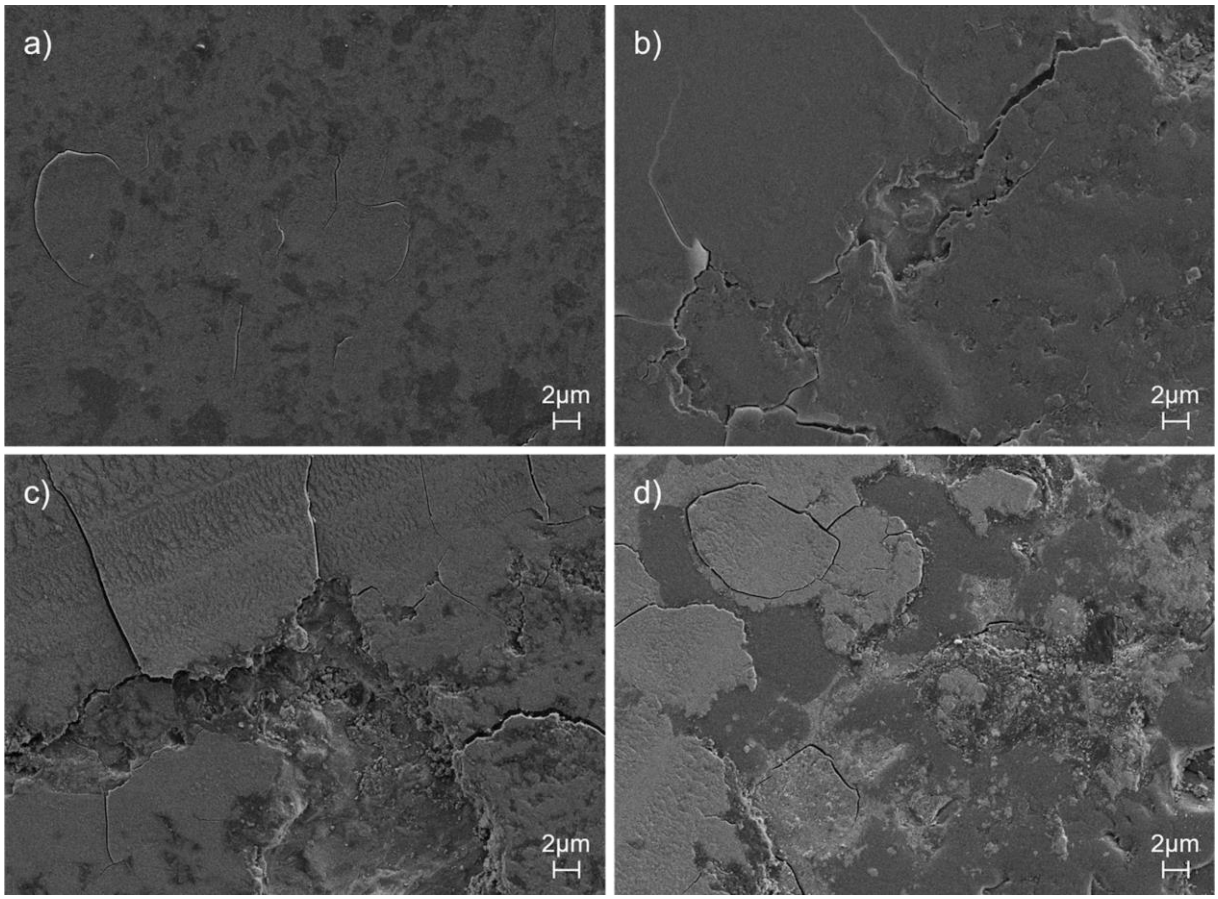

Fig. 6. FESEM micrographs of the worn surface of Al_2O_3-5vol.% NbC composites sintered by SPS at: a) 1450 ºC, b) 1500 ºC, c) 1550 ºC and d) 1600 ºC with 30 N of contact load.

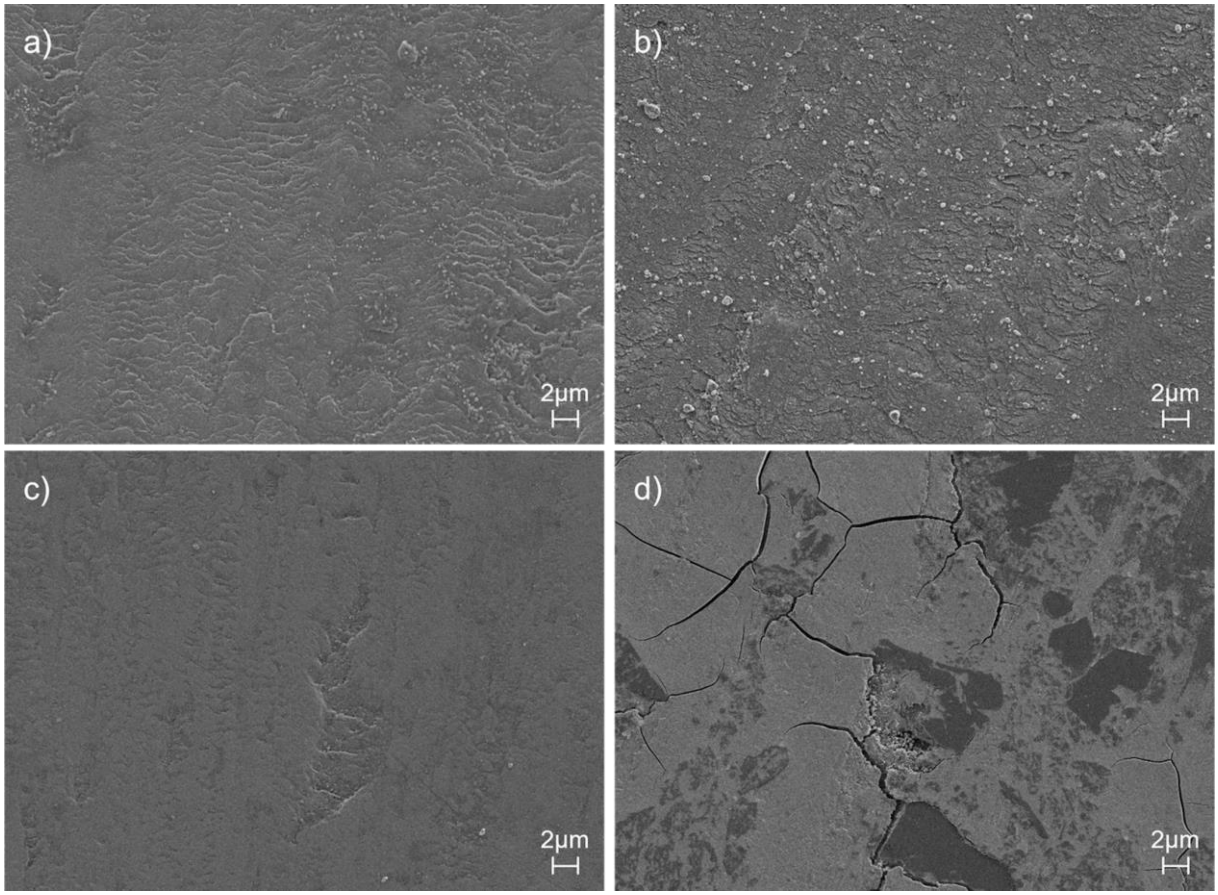

Fig. 7. FESEM micrographs of the worn surface of Al_2O_3-5vol.% NbC composites sintered by SPS at: a) 1450 ºC, b) 1500 ºC, c) 1550 ºC and d) 1600 ºC with 60 N of contact load.